INTERNATIONAL JOURNAL OF HEALTH & MEDICAL RESEARCH

ISSN(print): 2833-213X, ISSN(online): 2833-2148

Volume 02 Issue 09 September 2023

DOI : 10.58806/ijhmr.2023.v2i9n06

Page No. 289-295

Spatial Clustering Analysis of Dengue Hemorrhagic Fever in The First 9-Months of 2023 in Ho Chi Minh City, Vietnam

Huong-Giang Nguyen[1], Thi-Tuyet-Mai Nguyen[2]

[1,2] Faculty of Pharmacy, East Asia University of Technology, Hanoi, Vietnam

ABSTRACT:

Background: Dengue hemorrhagic fever is a notable vector-borne viral disease, currently becoming the most dreaded worldwide health problem in terms of the number of people affected. The objective of this study is to investigate spatial clustering of dengue hemorrhagic fever incidence in the first 9-months of 2023 in Ho Chi Minh city, Vietnam.

Methods: the global Moran's I statistic, Moran's I scatterplot and local statistic were employed to spatial clusters (high-high and low-low) and spatial outliers (low-high and high-low) in the study area of Ho Chi Minh city. The first and third order of contiguity were used to constructe spatial weight matrix.

Results: it was found from a case study of the first 9-months of 2023 in Ho Chi Minh city, a total of four high-high clusters, two low-low spatial clusters were detected in urban area and rural areas in the north and south of the Ho Chi Minh city, respectively when using the first order contiguity (statistically significance at the 0.05 level). For the case of using the third order of contiguity, a total of six high-low, two low-high spatial clusters and one low-low spatial cluster were successfully identified.

Conclusions: the study results has proven the effective use of the global Moran's I statistic, Moran's I scatterplot and local Moran's I statistic in the identification of spatial clustering of dengue hemorrhagic fever incidence.

KEYWORDS: Spatial Clustering, Dengue Hemorrhagic Fever, Local Moran's I, Ho Chi Minh city, Vietnam.

1. INTRODUCTION

Dengue is the leading cause of human arboviral disease worldwide. Dengue viruses (DENV) of the family Flaviviridae and genus Flavivirus, co-circulate as four antigenically related serotypes (DENV-1, −2, −3, and −4) (1). The clinical manifestations of dengue include dengue hemorrhagic, dengue hemorrhagic fever (DHF), and the most severe and potentially fatal dengue shock syndrome (2). It has been demonstrated that in endemic and hyper-endemic locations, more instances of dengue hemorrhagic fever develop from a dengue epidemic, which often correlates to more fatalities, especially if patients obtain medical care too late or the cases are managed inappropriately (3). However, because not all epidemics of dengue involve dengue hemorrhagic fever (4), it would help save lives if we knew the epidemiological conditions associated with the emergence of severe epidemics involving more dengue hemorrhagic fever cases and the overall risk patterns of total dengue cases (2).

By identifying the locations of outbreaks, disease mapping can efficiently target high-risk areas for early prevention and control (5,6) Geographical information systems (GIS) and statistical analysis of spatial characteristics of a disease have made it possible to identify clustering of cases and link the dynamics of the clustering with geographic locations that carry specific risk factors advantageous for the sources of infection (for example, mosquito breeding sites) and for the spread of infection (for example, vector exposure) (7–9). It is therefore, GIS techniques have been widely applied on disease mapping such as mapping the COVID-19 pandemic (10–12). For example, numerous efforts have been undertaken to examine the COVID-19 pandemic from a geographical viewpoint, such as the assessment of the COVID-19 hotspot in Kolkata, India, utilizing the Getis-Ord G statistic and regionally weighted principal component analysis to determine the effects of living environment deprivation (13). In order to analyze the regional and temporal differentiation characteristics and the contributing elements that influenced the COVID-19 epidemic spread in mainland China, exploratory spatial data analysis and the geodetector approach were also used (14). Another study in China looked at the COVID-19 pandemic's spatial clustering traits in Beijing using spatial autocorrelation analysis (15). Furthermore, spatial autocorrelation analysis has been successfully used in COVID-19 investigations in several nations, including the United States, to look into the spatiotemporal interaction effect of COVID-19 transmission (16), to determine the relationship between chronic air pollution and COVID-19 mortality in England (17), to investigate spatial autocorrelation patterns across five waves of COVID-19 in Catalonia, Spain (18), and to perform a spatiotemporal analysis of Italian COVID-19 outbreak (19). Moreover, studies using geographic information systems (GIS) have mapped the regional clustering patterns of dengue cases and examined the

relationships between these patterns and pertinent entomological parameters (6,20,21) and environmental conditions (22), and have determined the dengue and vector distributions' spatial-temporal diffusion patterns (21,23).

This study aimed to analyze the spatial clustering of dengue hemorrhagic fever incidence. The global Moran's I statistic, Moran's I scatterplot and local statistic will be employed to investigate spatial clusters (high-high and low-low) and spatial outliers (low-high and high-low) in Ho Chi Minh city. In addition, the first and third order of contiguity were also used to constructe spatial weight matrix in the identification of spatial clustering of dengue hemorrhagic fever.

2. MATERIALS AND METHODS

2.1. Materials

Data used in this study were collected in Ho Chi Minh City during the first 9 months of 2023. The number of dengue hemorrhagic fever cases per 100,000 population was shown in Figure 1. Data from Figure 1 shows districts with high number of cases were mainly concentrated in the city's administrative center. The districts with a high number of dengue hemorrhagic fever infections per 100,000 people include District 1 (154 cases with 45 cases/100.000 population), Phu Nhuan (125 cases with 47 cases/100.000 population), District 5 (90 cases with 44 cases/100.000 population), District 3 (80 cases with 36 cases/100.000 population), and District 11 (72 cases with 33 cases/100.000 population). Districts with low infection rates include Can Gio (67 cases with zero cases/100.000 population)), Nha Be (115 cases with 1 cases/100.000 population), and Binh Chanh (131 cases with 1 case/100.000 population).

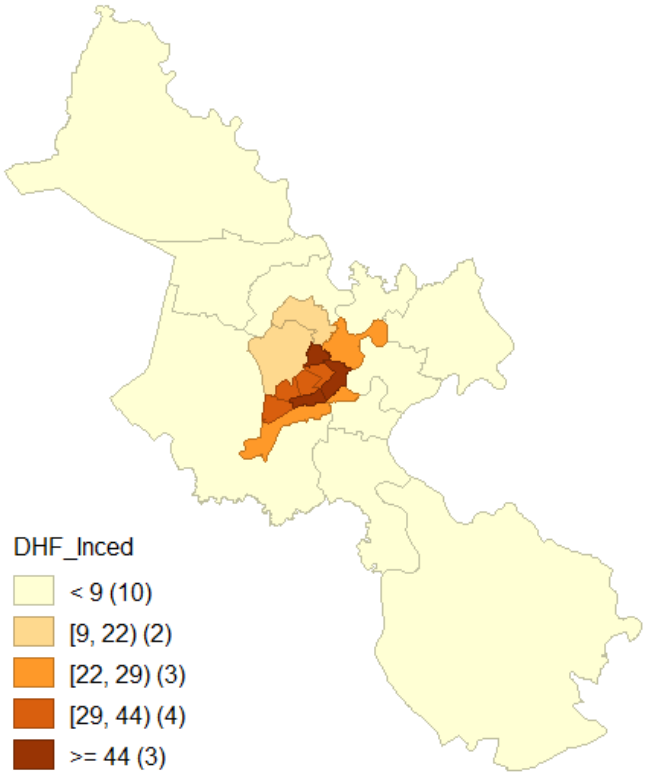

Figure 1. Map of dengue hemorrhagic fever incidence in 2023 in Ho Chi Minh city, Vietnam.

2.2. Methods

This study employed global Moran's I statistic to identify the spatial clustering of dengue hemorrhagic fever incidence at global scale (24,25). The definition of the global Moran's I statistic is expressed in equation (1):

$$I = \frac{n}{S_0}\frac{\sum_{i=1}^{n}\sum_{j=1}^{n} W_{ij}(x_i - \bar{x})(x_j - \bar{x})}{\sum_{i=1}^{n}\sum_{j=i}^{n} W_{ij}\sum_{i=1}^{n}(x_i - \bar{x})^2} \quad (1)$$

where x_i and x_j are the dengue hemorrhagic fever incidence for district i and district j; $\bar{x}$ is the mean of the dengue hemorrhagic fever incidence and be given by $\bar{x} = \sum_{i=1}^{n}\frac{x_i}{n}$; n is the total number of districts in the whole study area; and W_{ij} is a $(n \times n)$ spatial weight matrix (26).

The range of values of global Moran's I coefficient is in the interval [-1, +1] (26). Positive values of Moran's I result from the data's positive spatial autocorrelation, whereas Moran's I values are negative when there is a negative spatial autocorrelation (27). The absence of spatial autocorrelation or random in the distribution of dengue hemorrhagic fever incidence is shown by values of the global Moran's I coefficients that are near to zero.

The global Moran's I reflects the presence or lack of spatial autocorrelation as a whole. The regional Moran's I statistic was used to quantify the spatial clustering of low and high dengue hemorrhagic fever incidence in each district (26). The local Moran's I statistic (I_i) of dengue hemorrhagic fever incidence at district i is given by the following equation (28):

$$I_i = \frac{(x_i - \bar{x})}{\sigma^2} \sum_{j\#i, j\in J_i}^{N} W_{ij}(x_j - \bar{x}) \qquad (2)$$

where x_i, x_j, $\bar{x}$, and W_{ij} are defined in equation (1); N is the total number of neighborhood districts (26); J_i denotes the neighborhood set of dengue hemorrhagic fever incidence at district i; j#i implies that the sum of all $(x_j - \bar{x})$ of nearby neighbourhood districts of district i but not including x_j; and σ^2 is the variance of x, given in equation (3). W_{ij} defines neighbor connectivity and can be constructed using first order and third of contiguity (Figure 2).

$$\sigma^2 = \frac{1}{N}\sum_{j=1}^{N}(x_i - \bar{x}) \qquad (3)$$

The level of spatial clustering of dengue hemorrhagic fever incidence at each district is indicated by local Moran's I statistic. Similar to the global Moran's I statistic, the local Moran's I value at district i (I_i) also ranges between -1 and +1. There is no spatial autocorrelation of dengue hemorrhagic fever incidence if the local Moran's I coefficient at district i equals zero ($I_i = 0$). If $I_i > 0$ then there will be a positive spatial autocorrelation of dengue hemorrhagic fever incidence (26). If $I_i < 0$ then there will be a negative spatial autocorrelation of dengue hemorrhagic fever incidence. A high positive I_i shows the district i has a similarly high or low number of dengue hemorrhagic fever incidence cases as its neighbors and called the ''spatial cluster''(27). In this case, when there is a positive local spatial autocorrelation, the local Moran's I statistic indicates two types of spatial clusters for dengue hemorrhagic fever incidence cases, including: high-high spatial clusters and low-low spatial clusters. Low-high and high-low clusters are also two forms of spatial outliers that are identified using the local Moran's I statistic when there is a negative local spatial autocorrelation.

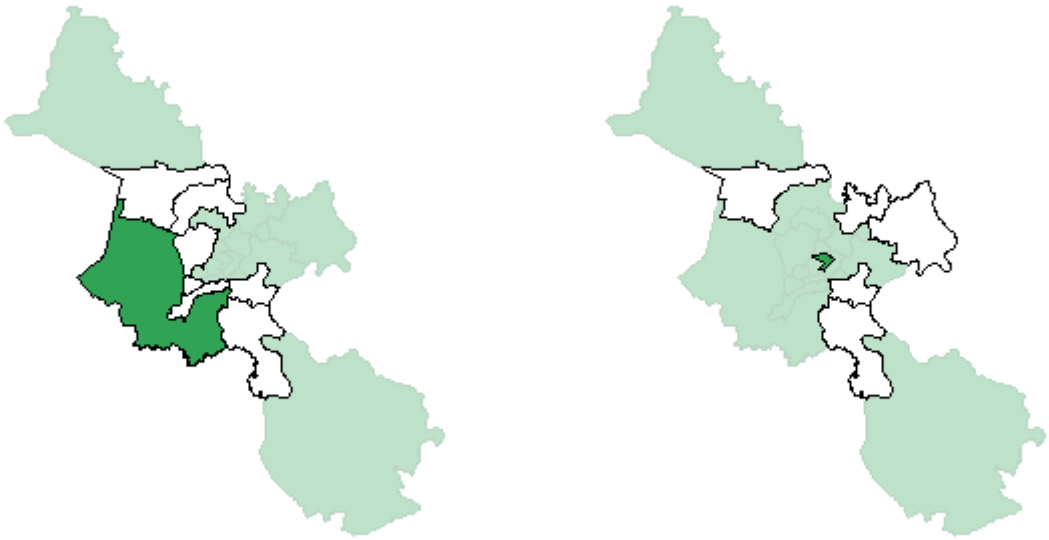

Figure 2. Map of neighbor connectivity using first order (left) and third (right) of contiguity in the study area of Ho Chi Minh city, Vietnam.

3. RESULTS AND DISCUSSIONS

3.1. Analysis of Moran's I scatterplot

Data from Moran scatter plots in Figure 3 illustrates the degree of globally spatial autocorrelation of dengue hemorrhagic fever in the case of using two different types of spatial weight matrices – the first and the third order of contiguity. The global Moran's I values were 0.559 and -0.420 corresponding with the use of the first order (Figure 3, left) and third order (Figure 3, right) of contiguity method, respectively. It was found that the first order method produces results with higer correlation coeffient when comparing with that of the first order method. This shows a higher degree of spatial autocorrelation between dengue hemorrhagic fever incidence for method of the first order of contiguity.

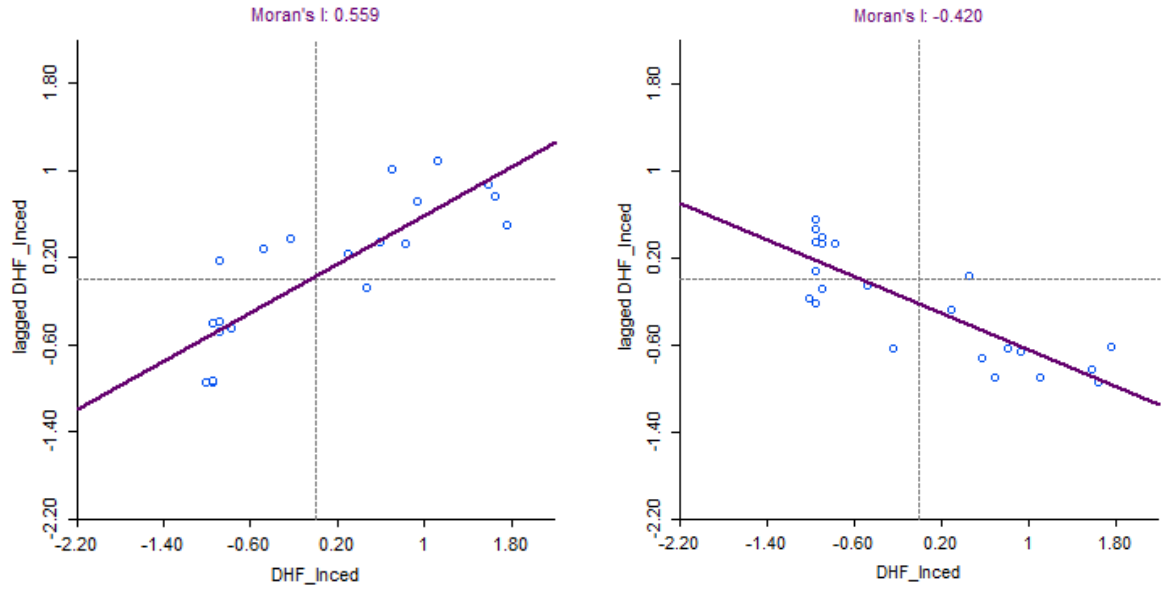

Figure 3. Moran's I scatterplots of dengue hemorrhagic fever incidence using first order (left) and third (right) of contiguity.

3.2. Analysis of spatial clustering of dengue fever incidence

Spatial clusters of dengue hemorrhagic fever incidence obtained from local Moran's I is shown in Figure 4 for the first order of contiguity,. Data from Figure 4 (left) shows that there were four high-high clusters, two low-low spatial clusters, no low-high and high-low spatial outliers, and 16 districts and town with unsignificant spatial clustering. In which, six high-high clusters were mainly distributed in the central area of Ho Chi Minh city where the population density is dense. Two low-low spatial clusters were distributed in rural areas in the north and south of the city. Data from Figure 4 (right) demonstrate that high-high and low-low spatial clusters were statistically significant with at the level of 0.05, of which five spaital clusters at the significant level of 0.05, four spatial clusters clusters at the significant level of 0.01 and only two spatial clusters at the significant level of 0.001. Both the left and right images in Figure 4 show that high-high spatial clusters were statistically significant at level of 0.01. These high-high spatial clusters were totally concentrated in four urban districts where a high number of dengue hemorrhagic fever incidence was confirmed in 2023 including District 1 (154 cases with 45 cases/100.000 population), District 3 (80 cases with 36 cases/100.000 population), District 5 (90 cases with 44 cases/100.000 population), and District 10 (70 cases with 29 cases/100.000 population). Two low-low spatial clusters were detected in sub-urban districts including Hoc Mon (68 cases with 01 case/100.000 population) and Nha Be (115 cases with 01 case/100.000 population).

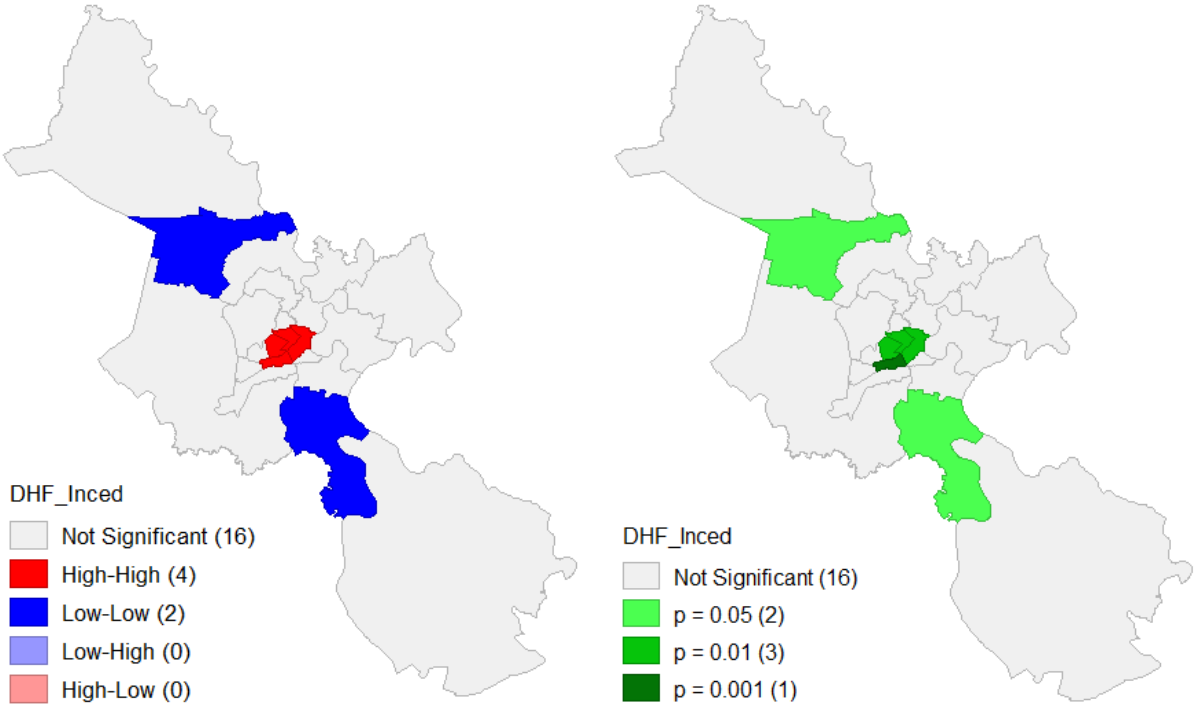

Figure 4. Spatial clustering of dengue hemorrhagic fever incidence using first order of contiguity: cluster map (left) and significance map (right).

Spatial clusters of dengue hemorrhagic fever incidence obtained from the third order method is shown in Figure 5. Contrary to those obtained from the case of using the first order of contiguity, data from Figure 5 data (left) shows that no high-high spatial clusters were detected. In this case, six high-low, two low-high spatial clusters and one low-low spatial cluster were successfully identified, in which 13 districts were found with statistical unsignificance. Six high-low clusters were mainly detected urban districts in the central area of Ho Chi Minh city. A low-low spatial clusters was also found in the centre of the city. Two low-high spatial clusters were mainly distributed in the suburban area of the north and south of the city. Data from Figure 5 (right) illustrates that one low-low spatial cluster, six high-low and two low-high spatial outliers were statistically significant at the level of 0.05, in which five clusters were statistically significant at the level of 0.05. Four clusters were statistically significant at the level of 0.01. And no high-high spatial clusters were detected at statistical significance of of 0.001. The spatial clustering of dengue hemorrhagic fever incidence from Figure 5 (left) illustrates that high-low spatial clusters were mainly concentrated in urban districts where high number of dengue hemorrhagic fever incidence were reported, including District 11 (72 cases with 33 cases/100.000 population), District 10 (70 cases with 29 cases/100.000 population), District 3 (80 cases with 36 cases/100.000 population), District 4 (58 cases with 27 cases/100.000 population), and District 5 (90 cases with 44 cases/100.000 population). Two low-high spatial outliers were in sub-urban districts including Hoc Mon (68 cases with 01 case/100.000 population) and Nha Be (115 cases with 01 case/100.000 population).

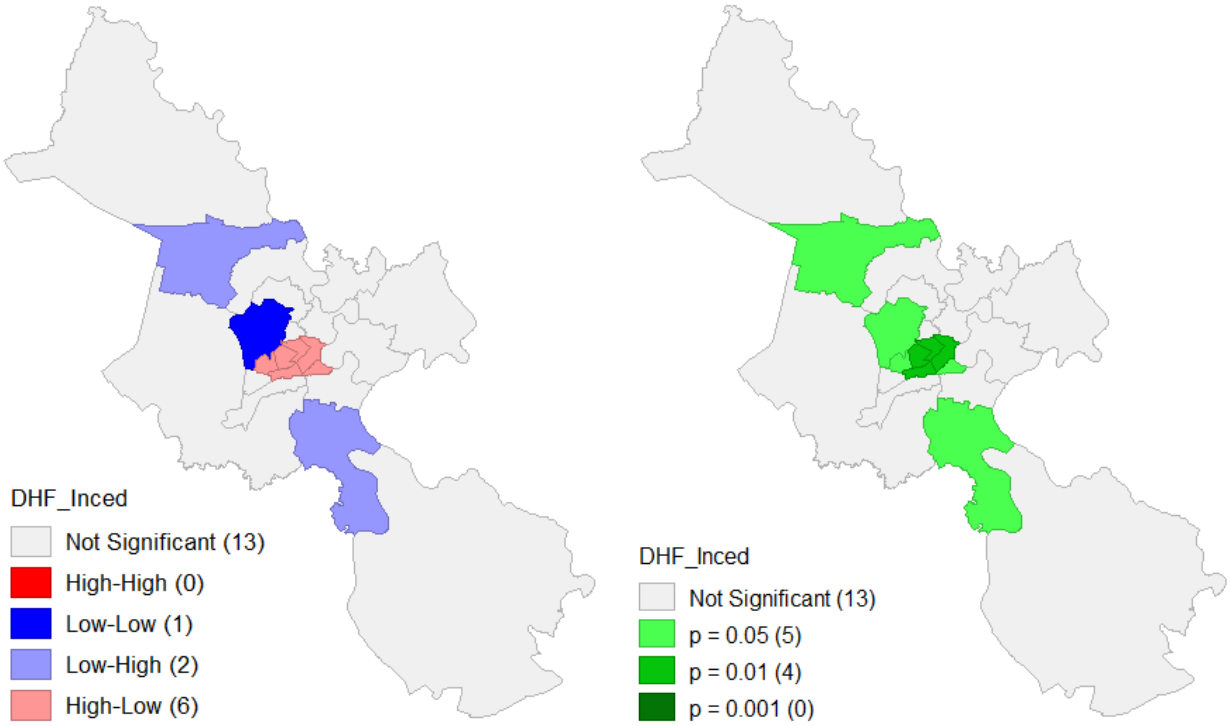

Figure 5. Spatial clustering of dengue hemorrhagic fever incidence using third order of contiguity: cluster map (left) and significance map (right).

4. CONCLUSIONS

This study is set out to investigate spatial clustering of dengue hemorrhagic fever incidence in 2023 in Ho Chi Minh city. Spatial clusters (high-high and low-low) and spatial outliers (low-high and high-low) was identified using the global Moran's I statistic, Moran's I scatterplot and local statistic. Additionally, the first and second order of contiguity were also employed to constructe spatial weight matrix. It was found from a case study of Ho Chi Minh city in 2023, when using the first order contiguity, four high-high clusters, two low-low spatial clusters were successfully detected in urban area and rural areas in the north and south of the Ho Chi Minh city, respectively. For the case of using the third order of contiguity, a total of six high-low, two low-high spatial clusters and one low-low spatial cluster were successfully identified. The study results has proven the effective use of the global Moran's I statistic, Moran's I scatterplot and local Moran's I statistic in the identification of spatial clustering of dengue hemorrhagic fever incidence.

DECLARATION BY AUTHORS

ETHICAL APPROVAL: Approved

ACKNOWLEDGEMENT: The authors would like to thank Ho Chi Minh Center for Disease Control (HoChiMinh CDC) for providing the data. The authors acknowledge the editors and anonymous reviewers for their insightful criticism and recommendations on this manuscript which helped to greatly improve the quality of the paper.

SOURCE OF FUNDING: None

CONFLICT OF INTEREST: The authors declare no conflict of interest

REFERENCES

1) Mammen Jr MP, Pimgate C, Koenraadt CJM, Rothman AL, Aldstadt J, Nisalak A, et al. Spatial and temporal clustering of dengue virus transmission in Thai villages. PLoS Med. 2008;5(11):e205.
2) Wen T-H, Lin NH, Chao D-Y, Hwang K-P, Kan C-C, Lin KC-M, et al. Spatial–temporal patterns of dengue in areas at risk of dengue hemorrhagic fever in Kaohsiung, Taiwan, 2002. Int J Infect Dis. 2010;14(4):e334–43.
3) Gubler DJ, Meltzer M. Impact of dengue/dengue hemorrhagic fever on the developing world. Adv Virus Res. 1999;53:35–70.
4) Trent D, Shin J, Hombach J, Knezevic I, Minor P, Group WHOW. WHO Working Group on technical specifications for manufacture and evaluation of dengue vaccines, Geneva, Switzerland, 11–12 May 2009. Vaccine. 2010;28(52):8246–55.
5) Snow J. On the mode of communication of cholera. The Commonwealth Fund. London: Oxford University Press; 1936.
6) Ali M, Wagatsuma Y, Emch M, Breiman RF. Use of a geographic information system for defining spatial risk for dengue transmission in Bangladesh: role for Aedes albopictus in an urban outbreak. Am J Trop Med Hyg. 2003;69(6):634–40.
7) Dunn CE, Kingham SP, Rowlingson B, Bhopal RS, Cockings S, Foy CJW, et al. Analysing spatially referenced public health data: a comparison of three methodological approaches. Health Place. 2001;7(1):1–12.
8) Cockings S, Dunn CE, Bhopal RS, Walker DR. Users' perspectives on epidemiological, GIS and point pattern approaches to analysing environment and health data. Health Place. 2004;10(2):169–82.
9) Lai PC, Wong C-M, Hedley AJ, Lo S V, Leung PY, Kong J, et al. Understanding the spatial clustering of severe acute respiratory syndrome (SARS) in Hong Kong. Environ Health Perspect. 2004;112(15):1550–6.
10) Shadeed S, Alawna S. GIS-based COVID-19 vulnerability mapping in the West Bank, Palestine. Int J Disaster Risk Reduct. 2021;64:102483.
11) Kamel Boulos MN, Geraghty EM. Geographical tracking and mapping of coronavirus disease COVID-19/severe acute respiratory syndrome coronavirus 2 (SARS-CoV-2) epidemic and associated events around the world: how 21st century GIS technologies are supporting the global fight against outbr. Vol. 19, International journal of health geographics. Springer; 2020. p. 1–12.
12) Utomo IC, Fadlilah U. Mapping of Covid-19 Vaccination Recipients in Sukoharjo Regency Based on Webgis. J Tek Inform. 2022;3(6):1773–81.
13) Das A, Ghosh S, Das K, Basu T, Dutta I, Das M. Living environment matters: Unravelling the spatial clustering of COVID-19 hotspots in Kolkata megacity, India. Sustain Cities Soc. 2021;65:102577.
14) Alves JD, Abade AS, Peres WP, Borges JE, Santos SM, Scholze AR. Impact of COVID-19 on the indigenous population of Brazil: A geo-epidemiological study. Epidemiol Infect. 2021;149:e185.
15) Han Y, Yang L, Jia K, Li J, Feng S, Chen W, et al. Spatial distribution characteristics of the COVID-19 pandemic in Beijing and its relationship with environmental factors. Sci Total Environ. 2021;761:144257.
16) Liu L, Hu T, Bao S, Wu H, Peng Z, Wang R. The spatiotemporal interaction effect of COVID-19 transmission in the United States. ISPRS Int J Geo-Information. 2021;10(6):387.
17) Huangfu P, Atkinson R. Long-term exposure to NO2 and O3 and all-cause and respiratory mortality: A systematic review and meta-analysis. Environ Int. 2020;144:105998.
18) Belvis F, Aleta A, Padilla-Pozo Á, Pericàs J-M, Fernández-Gracia J, Rodríguez JP, et al. Key epidemiological indicators and spatial autocorrelation patterns across five waves of COVID-19 in Catalonia. Sci Rep. 2023;13(1):1–11.
19) Ghosh P, Cartone A. A Spatio-temporal analysis of COVID-19 outbreak in Italy. Reg Sci Policy Pract. 2020;12(6):1047–62.
20) Tran A, Deparis X, Dussart P, Morvan J, Rabarison P, Remy F, et al. Dengue spatial and temporal patterns, French Guiana, 2001. Emerg Infect Dis. 2004;10(4):615.
21) Morrison AC, Getis A, Santiago M, Rigau-Perez JG, Reiter P. Exploratory space-time analysis of reported dengue cases during an outbreak in Florida, Puerto Rico, 1991-1992. Am J Trop Med Hyg. 1998;58(3):287–98.
22) Bohra A, Andrianasolo H. Application of GIS in Modeling Dengue Risk Based on Sociocultural Data: Case of Jalore, Rajasthan, India. 2001;
23) Ungchusak K, Burke DS. Travelling waves in the occurrence of dengue hemorrhagic fever in thailand. Nature.

2004;427:344347Cushing.

24) Cliff AD, Ord JK. Spatial processes: models & applications. (No Title). 1981;
25) Getis A, Ord JK. Local spatial statistics: An overview. Spatial analysis: Modeling in a GIS environment. Longley, P., and M. Batty. Wiley, New York; 1996.
26) Vu D-T, Nguyen T-T, Hoang A-H. Spatial clustering analysis of the COVID-19 pandemic: A case study of the fourth wave in Vietnam. Geogr Environ Sustain. 2021;14(4).
27) Nguyen TT, Vu TD. Identification of multivariate geochemical anomalies using spatial autocorrelation analysis and robust statistics. Ore Geol Rev. 2019;111.
28) Anselin L. Local indicators of spatial association—LISA. Geogr Anal. 1995;27(2):93–115.